Research Article

Crystal structure and molecular docking studies of octahydrocycloocta[b]pyridine-3-carbonitriles as potential inhibitors against *Mycobacterium tuberculosis*

RA Nagalakshmi[1], J Suresh[1], S Maharani[2] and R Ranjith Kumar[2]

[1]Department of Physics, The Madura College (Autonomous), Madurai, India
[2]Department of Organic Chemistry, School of Chemistry, Madurai Kamaraj University, Madurai, India

Received on August 14, 2014; Accepted on October 14, 2014; Published on October 31, 2014

Correspondence should be addressed to Janakiraman Suresh; E-mail: ambujasureshj@yahoo.com

Abstract

The compounds 1-benzyl-2-imino-4-p-tolyl-1,2,5,6,7,8,9,10-octahydrocycloocta[b]pyridine-3-carbonitrile (Ia) and 1-benzyl-2-imino-(4-methoxyphenyl-1,2,5,6,7,8,9,10-octahydrocycloocta {b]pyridine-3-carbonitrile (Ib) were synthesized. The crystal structures of the compounds were determined by single crystal X ray diffraction. The compounds C_{26} H_{27} N_3 (Ia**)** and C_{26} H_{27} N_3O **(**Ib**)** crystallize in the triclinic system (a = 10.2304(4) Å, b = 10.5655(4) Å, c = 11.8271(4) Å, α = 101.755(2) °, β = 106.934(2) °, γ = 114.071(2) ° and Z = 2 for I(a) and a = 10.2738(4) Å, b = 11.1654(5) Å, c = 11.4162(4) Å α = 98.549(2) °, β = 106.183(2) °, γ = 117.070(2) ° and Z = 2 for I (b)). In both compounds (Ia) and (Ib) the pyridine ring adopts a planar conformation and the cyclooctane ring adopts a twisted boat chair conformation. The synthesized compounds were screened for their antibacterial activities against the enzyme enoyl acyl carrier protein reductase, which is involved in the fatty acid biosynthesis of the mycobacterial cell wall. Both compounds showed good antibacterial activities. The synthesis of the compounds, their structure determination, their conformation, their intra- and intermolecular interactions and docking study results are given.

Introduction

Tuberculosis (TB) is an infectious disease caused by *Mycobacterium tuberculosis* and is the second leading cause of death in developing countries. Primary infection of *M. tuberculosis* takes place within the lungs but can involve any organ (Dietrich & Doherty 2009). Multidrug resistant tuberculosis and extensively drug-resistant tuberculosis have highlighted the deficiency of current standard treatment regimens. The bacterial drug resistance is mainly due to the slow growth, unusual cell envelope and genetic homogeneity (Besra *et al.* 1994). The cell wall of *M. tuberculosis* contains certain unique long chain (C70 to C90), α-alkyl and β-hydroxy fatty acids, referred to as mycolic acids. Its unusual lipid bilayer, formed by the latter, together with glycolipids and lipoprotein makes the cell wall tough, and the drugs normally used for the treatment of the infection, partially effective (Pieters 2008). Hence, there is a need to develop new drug candidates which have anti-mycobacterial activity.

The heterocycles containing nitrogen show good anti-mycobacterial activities (Sriram *et al.* 2006). Many naturally occurring and synthetic compounds containing the pyridine scaffold show important pharmacological properties (Temple *et al.* 1992). Cyanopyridine derivatives possess anti-microbial activities (Dandia *et al.* 1993). As a continuation of our work for developing new drugs for *M. tuberculosis* (Suresh *et al.* 2012), the 1-benzyl-2-imino-4-p-tolyl-1,2,5,6,7,8,9,10-octahydrocycloocta[b]pyridine-3-carbonitrile (Ia) and 1-benzyl-2-imino-(4-methoxyphenyl-1,2,5,6,7,8,9,10-octahydrocycloocta[b] pyridine-3-carbonitrile (Ib) compounds were synthe-

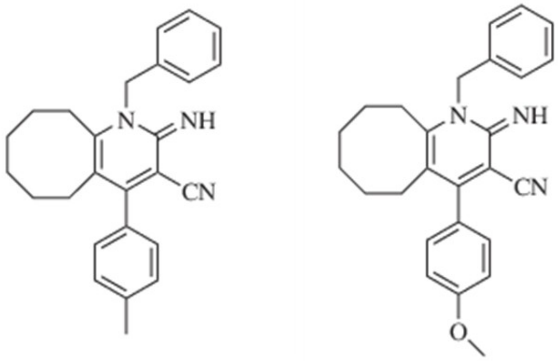

Figure 1. Chemical diagram of the molecule (Ia) (left) and (Ib) (right).

Table 1. The crystal data, intensity data collection, structure solution and structure refinement parameters of compounds (Ia) and (Ib).

Empirical formula	$C_{26}H_{27}N_3$	$C_{26}H_{27}N_3O$
Formula weight	381.51	397.51
Temperature	293(2) K	293(2) K
Wavelength	0.71073 Å	0.71073 Å
Crystal system /space group	Triclinic/P-1	Triclinic/ P-1
Unit cell dimensions	a = 10.2304(4) Å	a = 10.2738(4) Å
	b = 10.5655(4) Å	b = 11.1654(5) Å
	c = 11.8271(4) Å	c = 11.4162(4) Å
	a = 101.755(2)°	a = 98.549(2)°
	b = 106.934(2)°	b = 106.183(2)°
	g = 114.071(2)°	g = 117.070(2)°
Volume	1037.69(7) Å3	1060.20(7) Å3
Z/ Density (calculated)	2/ 1.221 Mg/m3	2/1.245 Mg/m3
Absorption coefficient	0.072 mm-1	0.077 mm-1
F(000)	408	424
Crystal size	0.21x0.19 x0.18 mm3	0.21 x 0.19 x 0.18 mm3
Theta range for data collection	2.27 to 25.50°.	2.16 to 25.49°.
Limiting indices	-12<=h<=12, -12<=k<=12, -14<=l<=14	-12<=h<=12, -13<=k<=13, -13<=l<=13
Reflections collected	23565	25081
Independent reflections	3865 [R(int) = 0.0272]	3947 [R(int) = 0.0302]
Completeness to theta = 25.50°	100.0 %	99.9 %
Refinement method	Full-matrix least-squares on F2	Full-matrix least-squares on F2
Data / restraints / parameters	3865 / 2 / 268	3947 / 16 / 311
Goodness-of-fit on F2	1.052	1.035
Final R indices [I>2sigma(I)]	R1 = 0.0453, wR2 = 0.1175	R1 = 0.0474, wR2 = 0.1258
R indices (all data)	R1 = 0.0710, wR2 = 0.1335	R1 = 0.0761, wR2 = 0.1463
Extinction coefficient	0.020(3)	0.034(4)
Largest diff. peak and hole	0.275 and -0.177 e.Å-3	0.197 and -0.238 e.Å-3

sized and their structural characteristics were studied using single crystal X-ray diffraction. Furthermore, they were screened for anti-mycobacterial activities using Autodock.

Synthesis

Preparation of compound (Ia)

A mixture of cyclooctanone (1 mmol), 4-methyl benzaldehyde (1 mmol) and malononitrile (1 mmol) were taken in ethanol (10 mL); *p*TSA (0.5 mmol) was subsequently added. The reaction mixture was heated under reflux for 2-3 h. After completion of the reaction (TLC), the reaction mixture was poured into crushed ice and extracted with ethyl acetate. The excess solvent was removed under vacuum and the residue was subjected to column chromatography using petroleum ether/ethyl acetate mixture (97:3 v/v) as eluent to afford pure product. The pure product was crystallized using ethyl acetate, as solvent. The melting point was 501 K and the yield was 69%.

Preparation of compound (Ib)

A mixture of cyclooctanone (1 mmol), 4-methoxy benzaldehyde (1 mmol) and malononitrile (1 mmol) were taken in ethanol (10 mL); *p*TSA (0.5 mmol) was subsequently added. The reaction mixture was heated under reflux for 2-3 h. After completion of the reaction (TLC), the reaction mixture was poured into crushed ice and extracted with ethyl acetate. The excess solvent was removed under vacuum and the residue was subjected to column chromatography using petroleum

ether/ ethyl acetate mixture (97:3 v/v) as eluent to afford pure product. The pure product was crystallized using ethyl acetate, as solvent. The melting point was 511 K and the yield was 70%.

Structure Determination and Refinement

Single crystals of suitable sizes of both compounds were selected for crystal structure determination. The intensity data of the crystals were collected using a Bruker AXS Kappa APEX II single crystal CCD Diffractometer equipped with graphite-monochromated MoKα radiation (λ=0.71073Å) at room temperature. The data collection, data reduction and absorption corrections were carried out using the APEX2, SAINT-Plus and SADABS programs (Bruker 2004). The trial structures of both the compounds were obtained using SHELXL-97. The structures were refined by the full-matrix least-squares method using SHELXL-97 (Sheldrick 2008). The non-hydrogen atoms were also refined with independent anisotropic displacement parameters using the same program (Sheldrick 2008). The NH hydrogen atoms were located from a difference Fourier map and refined isotropically. The other H atoms were placed in calculated positions and allowed to ride on their carrier atoms with C---H = 0.93 Å (aromatic CH), 0.96 Å (methyl CH_3) or 0.97 Å (methylene CH_2), and N---H = 0.86 Å. Isotropic displacement parameters for H atoms were calculated as Uiso = $1.5U_{eq}$(C) for CH_3 groups and U_{iso} = $1.2U_{eq}$ (carrier atom) for all other H atoms. The methoxy substituted molecule was disordered. The carbon atoms C8 and C9, with their corresponding hydrogen atoms of the cyclooctane ring of the compound (Ib) are disordered with occupancy factors 0.33485:0.60186, respectively. The disordered carbon atoms of the cyclooctane ring were refined using SHELXL-97 (Sheldrick 2008).

Docking Studies

Isoniazid (INH) was initially found to be active against tuberculosis in 1952, while its mode of action was still unknown (Bernstein *et al*. 1952, Fox 1952). It was later shown that INH inhibits the biosynthesis of mycolic acid, that covers the surface of mycobacteria (Takayama *et al*. 1972). There is strong evidence that this is the pathway that exerts the main effect of INH treatment (Winder 1982, Quemard *et al*. 1991). Using gene transfer systems for mycobacteria, a gene called InhA was identified as a target for INH (Banerjee *et al*. 1994). These studies revealed that InhA preferentially catalyzes the NADH-dependent reduction of 2-*trans*-enoyl-ACP molecules with 16 or more carbons (Dessen *et al*. 1995, Quemard *et al*. 1995). This serves as the last step in fatty acid elongation. Despite the increasing numbers of primary and secondary resistance, isoniazid remains one of the key drugs to treat tuberculosis (Cohn *et al.* 1997). Further studies show that INH can penetrate the mycobacterial envelope through passive diffusion; it then inhibits the InhA enzyme by covalently attaching to NADH within the protein active site (Rozwarski *et al*. 1998). Additionally, inhibition of InhA blocks mycolic acid biosynthesis, eventually leading to cell death (Vilcheze *et al*. 2000). The enoyl-acyl carrier protein reductase from *Mycobacterium tuberculosis* (InhA) is a fundamental target for antituberculosis intervention (Dessen *et al.* 1995, Rozwarski *et al.* 1998).

Nowadays, even though the antibacterial effects of isoniazid and triclosan (a newer InhA inhibitor) establish the suitability of the target for drug intervention, these compounds themselves have several limitations, including resistance and suboptimal bioavailability (Wang *et al.* 2004). Here, we report a new chemically distinct series, 1-benzyl-2-imino-4-(4-methylphenyl)-1, 2,5,6,7,8,9,10-octahydrocycloocta[b]

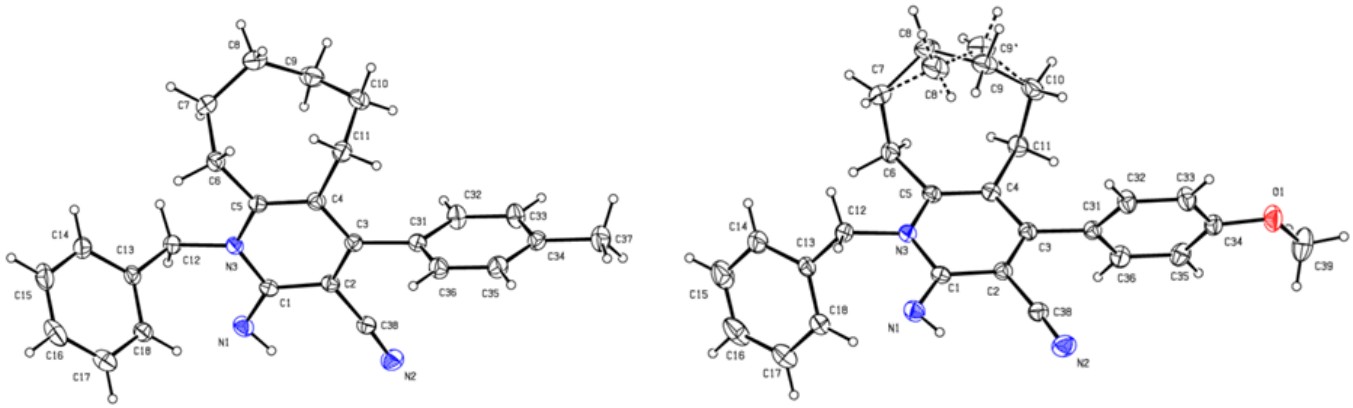

Figure 2. The molecular structure of compounds **(**Ia**)** (left) and (Ib**)** (right), showing the atom numbering scheme. Displacement ellipsoids are drawn at 20% probability level, using Platon (Spek 2008).

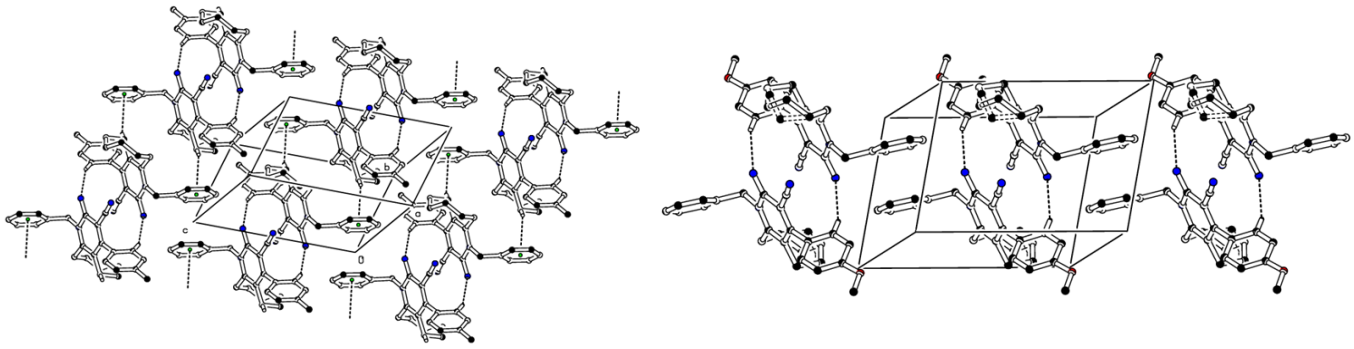

Figure 3. The inversely related molecules form a ring motif; they are further linked through C-H…π (left) and van der walls (right) interactions in the case of compound (Ia) (left) and (Ib) (right).

pyridine-3-carbonitrile, which has anti-mycobacterial activity. We have attempted, aided by a docking approach, to elucidate the extent of specificity of enoyl acyl carrier protein towards synthesized compounds, as anti-tubercular agents. The coordinates of enoyl acyl carrier protein (2NSD) with Nad were then retrieved from the RCSB protein data bank (http://www.pdb.org). The protein structure was cleaned using the whatif online server. Enoyl acyl carrier protein's active site pocket was identified using the online server Computed Atlas of Surface Topography (CASTp). The preparation of the protein and ligand input structures and the definition of the binding sites were carried out under a GRID-based procedure. A rectangular grid box was constructed over the protein with grid points 90X90X90 $Å^3$ separated by 0.375 Å under the docking procedure. The lowest energy cluster returned by AutoDock for each compound was considered and used for further analysis. Consequently runs were setup to 100 for each inhibitor. All other parameters were maintained at their default settings. All docking result visualizations are depicted using the PDBsum online server.

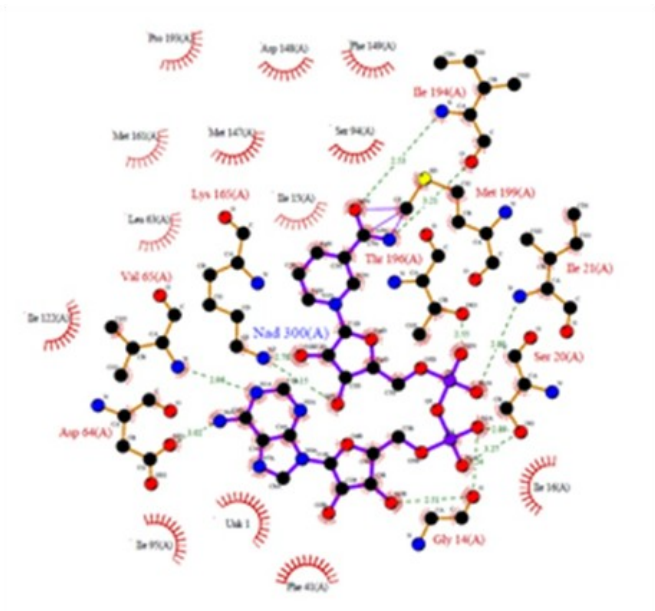

Figure 4. Enoyl acyl carrier protein reductase interactions for compound (Ia).

Results and Discussion

The molecular structures of compounds (Ia) and (Ib) are shown in Figure 2. In both compounds, the cyclooctane ring adopts a twisted boat-chair conformation. The pyridine ring is planar with an r.m.s. deviation of 0.0041 (1) Å in (Ia) and 0.0085 (1) Å in (Ib). The N1 atom is deviating by -0.0446 (1) Å from the mean plane of the pyridine ring in compound (Ia) and 0.393 (1) Å in compound (Ib). The aromatic ring (C31-C36) and phenyl rings (C13-C18) are planar with an r.m.s. deviation of 0.0059 Å and 0.0070 Å in compound (Ia) and in compound (Ib). The sum of the angles around atom N3 (360°) indicates that the atom N3 is in sp^2 hybridization in both compounds. The nitrile atoms C38 and N2 are displaced from the mean plane of the pyridine ring by 0.0384(1) Å and 0.0612(1) Å, respectively, in compound (Ia) and -0.0090(1) Å and 0.0050(1) Å, in compound (Ib). The methyl benzene ring attached to the pyridine ring is in an (-) anti-clinal conformation with torsion angle C2--C3--C31--C36 = -98.5(2) ° in compound (Ia) and in an (+) anti-clinal conformation with torsion angle C2--C3--C31--C36 = 99.8(2) ° in compound (Ib). The torsion angle C32--C34--C33--C37 = -179.3° (2) indicates the methyl carbon atom attached to the benzene ring is in an (-) anti peri planar conformation in compound (Ia). The plane formed by the cyano group is twisted away from the plane of pyridine ring in both compounds; 50.42 (1)° in compound (Ia) and 36.20 (1)° in compound (Ib).

Crystal Packing

In the crystal structure of the compound (Ia**)** the atom C32 of the aryl ring is involved in the intermolecular

Table 2. Hydrogen bonds [Å and °] of compound (Ia). Cg1 is the centroid of the (C13-C18) phenyl ring.

D-HA	d(D-H)	...d(HA)	...d(DA)	<DHA
C(32)-H(32)...N(1)$^{(i)}$	0.93	2.61	3.473(2)	154
C(11)-H(11)...Cg1$^{(ii)}$	0.97	2.93	3.583(2)	126

Symmetry transformations used to generate equivalent atoms:
(i) (- x, - y, 1 – z)
(ii) (1 - x,1 - y,1 – z)

interaction C32—H32···N1$^{(i)}$ (with the N1 atom) and forms a ring motif $R_2^2(14)$ (Bernstein *et al.* 1995) along the b axis [symmetry code: (i) (- x, - y, 1 – z)]. These adjacent ring motifs are linked together by C-H…π $^{(ii)}$ interactions [symmetry code: (ii) (1 - x, 1 - y, 1 – z)], (Figure 3). Furthermore, in the crystal structure of compound (Ib**)** the intermolecular interaction C32—H32···N1$^{(i)}$ with the N1 atom forms a ring motif R_2^2 (14) (Bernstein *et al.* 1995) along the b-axis [symmetry code: (i) (1 - x, 1 - y, 1 – z)]. These adjacent ring motifs are linked together by van der Walls interactions (Figure 3).

The C—N distance is longer [3.473 (3) Å] in compound (Ia) than in compound (Ib) [3.465 (3) Å] even though the C—H···N angle [154 (2) °, 154 (17) °] is similar in both structures. This shows that the 4-methoxy substituent forms a stronger hydrogen bond than the methyl substituent. The intermolecular hydrogen bond geometry of compound (Ia) and compound (Ib) is listed in Table 2.

Docking analysis

The target protein structure of 2NSD with Nad was docked with the synthesized compounds using AutoDock4 version 2 (Goodsell 1998). The target protein contains two monomers. Only one monomer was selected for docking studies (Figure 4).

Table 3. Hydrogen bonds [Å and °] of compound (**Ib**)

D-HA	d(D-H)	...d(HA)	...d(DA)	<DHA
C(18)-H(18)...N(1)	0.93	2.61	3.284(3)	130
C(32)-H(32)...N(1)$^{(i)}$	0.93	2.60	3.464(3)	154

Symmetry transformation used to generate equivalent atoms:
(i) (1 - x, 1 - y, -z)

The synthesized compounds were found to display good binding affinity to the receptor as shown in Table 3 and in Figure 6, with minimum binding energy. From Table 4, it was found that the stabilized binding interactions of our compounds are due the strong influence from the VDW + Hbond + desolv energy, than the electrostatic interactions.

The hydrophobic pocket of InhA is flexible whereas its hydrophilic pocket appears more rigid for the binding of inhibitors (Punkvang *et al.* 2010). InhA inhibitors may interact with its hydrophilic pocket formed by the backbone of Gly ^{96}, Phe ^{97} and Met ^{98}. Hydrophobicity is favourable for the MIC value but its appears to be unfavorable for the activity against *M. tuberculosis*. Hence, there should be a fine balance between the hydrophobic and hydrophilic properties of direct InhA inhibitors, to ensure their effectiveness against both InhA and *M. tuberculosis*. These structural requirements are favorable not only for MIC values but also assist the binding of InhA inhibitors in the hydrophilic InhA pocket. The key structural feature of such InhA inhibitors should be taken. Thus, having a bulky group encompassing suitable hydrophobic and hydrophilic properties could improve the MIC value of direct InhA inhibitors.

In compound (Ia), the nitrogen atom of the pyridine ring is hydrogen bonded to GLY ^{96}, one of the catalytic residues in the InhA active site. The hydrogen bond is formed in the hydrophilic pocket and has hydrophobic interactions with the hydrophobic pocket. Hence it shows good anti-mycobacterial activity.

Rozwarski *et al.* (1999) determined the crystal structure of InhA with a C fatty acyl substrate; they reported that hydrophobic amino acids of the loop are important for substrate binding into the cavity. Of note, the last few carbon atoms of the substrate were shown to interact with Ala^{198}, Met^{199}, and Ile^{202}, which are all hydrophobic. A fatty acid shorter than 16 carbons might not fit well in the enzyme, as there will be missing interactions with Ala^{198}, Met ^{199}, and Ile^{202}. There is strong evidence that the interactions with the three amino acids are important determinants for loop ordering. Our inhibitor (Ib) is able to directly interact with one of these residues (Ala^{198}), generating a defined loop structure and having hydrophobic interactions to the important loop residues of InhA, leading to a slow tight binding inhibition. Inhibitor residence time is an important factor for *in vivo* drug activity (Lavie *et al.* 1997, Lewandowicz *et al.* 2003, Tummino *et al.* 2008). Slow onset inhibitors will spend a

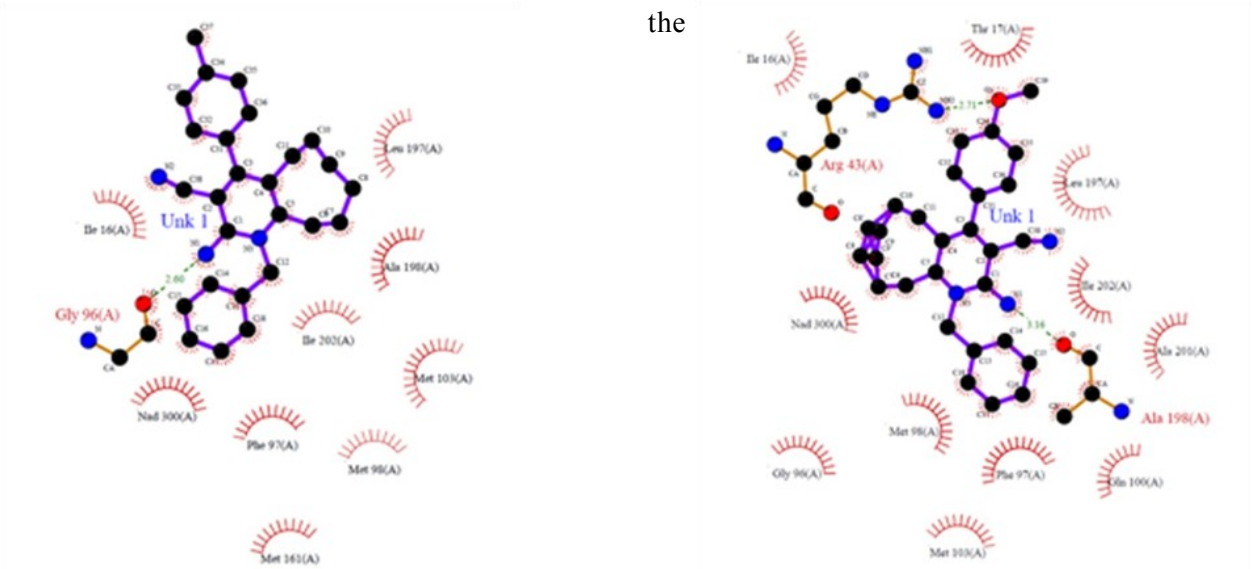

Figure 5. Interactions of compound (Ia) (left) and compound (Ib) (right) with enoyl acyl carrier protein.

longer time bound to their target molecules and can remain bound even at low free drug concentrations. In this regard, our inhibitor (Ib) shows the features of slow onset inhibitors.

Conclusion

For our goal to propose new inhibitors, we synthesized two compounds of pyridine derivatives. The compounds were docked and their binding free binding energies were evaluated. Both compounds show good binding affinity with acceptable free binding energy which indicates that they give good stable complexes. Hence our synthesized ligands show good antitubercular activities. From the docking analysis of the two compounds with the receptor of enoyl acyl carrier protein it was found that (Ib) shows better binding with the receptor, as compared to (Ia).

Conflict of interest

The authors declare no conflicts of interest.

Supplementary Material

Crystallographic data (excluding structure factors) for the structures of (Ia) and (Ib) reported in this paper have been deposited with the Cambridge Crystallographic data Centre as supplementary publication CCDC 1017700 & CCDC 1017701. Copies of the data can be obtained, free of charge, on application to, CCDC, 12 Union Road, Cambridge, and CB2 1 EZ UK; Fax: 044-1223-336033; Email: deposit@ccdc.cam.uk or at http://www.ccdc.cam.ac.uk/.

Acknowledgements

JS thanks the UGC for the FIST support. JS and RAN thank the management of The Madura College (Autonomous), Madurai for their encouragement and support. RRK thanks University Grants Commission, New Delhi, for funds through Major Research Project F. No. 42-242/2013 (SR). SM thanks the university grants commission, New Delhi for the fellowship under UGC-BSR-JRF meritorious scheme.

Conflicts of interest

The authors have no conflicts of interest.

Table 4. Binding energy of compounds (Ia) and (Ib).

Ligand	Binding Energy (Kcal/mol)	Intermolecular Energy (Kcal/ mol) (A+B)	VDW + Hbond + desolv energy (Kcal/ mol) (A)	Electrostatic energy (Kcal/ mol) (B)
Ia	-7.83	-9.03	-9.02	-0.01
Ib	-8.67	-10.16	-9.93	-0.23

References

Banerjee A, Dubnau E, Quemard A, Balasubramanian V, Um KS, Wilson T, Collins D, de Lisle G & Jacobs WR Jr 1994 inhA, a gene encoding a target for isoniazid and ethionamide in Mycobacterium tuberculosis. *Science* **263** 227-230

Besra GS & Chatteriee D 1994 Lipids and carbohydrate of Mycobacterium tuberculosis. In *Tuberculosis: Pathogenesis, Protection, and Control*, pp 285-306. Eds BR Blood. Washington, DC: ASM Press

Bernstein J, Lott WA, Steinberg BA & Yale HL 1952 Chemotherapy of experimental tuberculosis. *Am Rev-Tuberc* **65** 357-374

Bernstein J, Davis RE, Shimoni L & Chang NL 1995 Patterns in Hydrogen Bonding: Functionality and Graph Set Analysis in Crystals. *Angew Chem Int Ed Engl* **34** 1555-1573

Blanchard JS 1995 Enzymatic characterization of the target for isoniazid in Mycobaterium tuberculosis. *Biochemistry* **34** 8235-8241

Bruker 2004 APEX2 and SAINT. Bruker AXS Inc., Madison, Wisconsin, USA

Cohn DL, Bustreo F & Raviglione MC 1997 Drug-resistant tuberculosis: review of the worldwide situation and the WHO/IUATLD global surveillance project. *Clin Infect Dis* **24** S121-S130

Dandia A, Sehgal V & Singh P 1993 Synthesis of fluorine containing 2-aryl-3-pyrazolyl/pyranyl/isoxazolinyl -indole derivatives as antifungal and antibacterial agents. *Indian J Chem* **32** 1288-1291

Dessen A, Quemard A, Blanchard JS, Jacobs WR & Sacchettini JC 1995 Crystal structure and function of the isoniazid target of Mycobacterium tuberculosis. *Science* **267** 1638-1641

Dietrich J & Doherty TM 2009 Interaction of Mycobacterium tuberculosis with the host: consequences for vaccine development *APMIS* **117** 440-457

Lavie A, Vetter IR, Konrad M, Goody RS, Reinstein J & Schlichting I 1997 Structure of thymidylate kinase reveals the cause behind the limiting step in AZT activation. *Nat Struct Biol* **4** 601-604

Lewandowicz A, Tyler PC, Evans GB, Furneaux RH & Schramm VL 2003 Achieving the ultimate physiological goal in transition state analogue inhibitors for purine nucleoside phosphorylase. *J Biol Chem* **278** 31465-31468

Goodsell DS, Morris GM & Olson AJ 1998 Automated docking of flexible ligands: Applications of autodock *J Mol Recog* **9** 1-5

Pieters J 2008 *Mycobacterium tuberculosis* and the macrophage: Maintaining a Balance. *Cell Host Microbe* **3** 399-407

Punkvang A, Saparpakorn P, Hannongbua S, Wolschann P, Beyer A & Pungpo P 2010 Investigating the structural basis of arylamides to improve potency against M. tuberculosis strain through molecular dynamics simulations. *Eur J Med Chem* **45** 5585-5593

Rajni & Meena LS 2011 Unique characteristic features of *Mycobacterium tuberculosis* in relation to immune system. Am. J Immunol **7** 1-8

Rozwarski DA, Grant GA, Barton DH, Jacobs WR Jr & Sacchettini JC 1998 Modification of the NADH of the isoniazid target (InhA) from Mycobacterium tuberculosis. *Science* **279** 98-102

Rozwarski DA, Vilchèze C, Sugantino M, Bittman R & Sacchettini JC 1999 Crystal structure of the Mycobacterium tuberculosis enoyl-ACP reductase, InhA, in complex with NAD+ and a C16 fatty acyl substrate. *J Biol Chem* **274** 15582-15589

Sheldrick GM 2008 A short history of *SHELX*. *Acta Cryst* A **64** 112-122

Sriram D, Yogeeswari P & Madhu K 2006 Synthesis and in Vitro Antitubercular Activity of Some 1-[(4-sub) Phenyl]-3-(4-{1-[(Pyridine-4 Carbonyl) Hydrazono] Ethyl}Phenyl)Thiourea. *Bioorg Med Chem Lett* **16** 876-878

Spek AL 2009 Structure validation in chemicalcrystallography. *Acta Cryst* D **65** 148-155

Suresh J, Vishnu Priya R, Sivakumar S & Ranjith Kumar R 2012 Spectral analysis and crystal structure of two substituted spiro acenaphthene structures *J Mol Biochem* **1** 183-188

Takayama K, Wang L & David HL 1972 Effect of isoniazid on the in vivo mycolic acid synthesis, cell growth, and viability of *Mycobacterium tuberculosis*. *Antimicrob Agents Chemother* **2** 29-35

Temple C, Rener GA, Raud WR & Noker PE 1992 Antimitotic agents: structure-activity studies with some pyridine derivatives. *J Med Chem* **35** 3686-3690

Tummino PJ & Copeland RA 2008 Residence time of receptor-ligand complexes and its effect on biological function. *Biochemistry* **47** 5481-5492

Quémard A, Lacave C & Lanéelle G 1991 Isoniazid inhibition of mycolic acid synthesis by cell free extracts of sensitive and resistant strains of *Mycobacterium aurum*. *Antimicrob Agents Chemother* **35** 1035-1039

Quemard A, Sacchettini JC, Dessen A, Vilcheze C, Bittman R, Jacobs WR Jr & Blanchard JS 1995 Enzymatic characterization of the target for isoniazid in *Mycobaterium tuberculosis*. *Biochemistry* **34** 8235-8241

Vilcheze C, Morbidoni HR, Weisbrod TR, Iwamoto H, Kuo M, Sacchettini JC & Jacobs WR Jr 2000 Inactivation of the inhA-encoded fatty acid synthase II (FASII) enoyl-acyl carrier protein reductase induces accumulation of the FASI end products and cell lysis of Mycobacterium smegmatis. *J Bacteriol* **182** 4059-4067

Wang LQ, Falany CN & James MO 2004 Triclosan as a substrate and inhibitor of 3'-phosphoadenosine 5'-phosphosulfate-sulfotransferase and UDP-glucuronosyl transferase in human liver fractions. *Drug Metab Dispos* **32** 1162-1169

Winder FG 1982 Mode of action of the antimycobacterial agents. In *The Biology of the Mycobacteria*, vol. 1, pp. 353-438. Edited by C. Ratledge & J. Stanford. London: Academic Press

Winder FG & Collins PB 1970 Inhibition by isoniazid of synthesis of mycolic acids in *Mycobacterium tuberculosis*. *J Gen Microbiol* **63** 41-48